

On Holographic Entanglement Entropy of Charged Matter

Manuela Kulaxizi¹, Andrei Parnachev² and Koenraad Schalm²

¹ Université Libre de Bruxelles and International Solvay Institutes,
ULB Campus Plaine CP231, B-1050 Bruxelles, Belgium

²Institute Lorentz for Theoretical Physics, Leiden University
P.O. Box 9506, Leiden 2300RA, The Netherlands

We study holographic entanglement entropy in the background of charged dilatonic black holes which can be viewed as holographic duals of certain finite density states of $\mathcal{N} = 4$ super Yang-Mills. These charged black holes are distinguished in that they have vanishing ground state entropy. The entanglement entropy for a slab experiences a second order phase transition as the thickness of the slab is varied, while the entanglement entropy for a sphere is a smooth function of the radius. This suggests that the second scale introduced by the anisotropy of the slab plays an important role in driving the phase transition. In both cases we do not observe any logarithmic violation of the area law indicative of hidden Fermi surfaces. We investigate how these results are affected by the inclusion of the Gauss-Bonnet term in the bulk gravitational action. We also observe that such addition to the bulk action does not change the logarithmic violation of the area law in the backgrounds with hyperscaling violation.

1. Introduction and summary

Understanding strongly interacting compressible states of matter has been a subject of intense research (see e.g. [1] for a recent review). In this pursuit, it is natural to use the AdS/CFT correspondence, which provides an analytic machinery of dealing with strongly interacting field theoretic systems. A natural route involves starting with the well-understood duality between the $\mathcal{N} = 4$ Super Yang Mills in $3+1$ dimensions and type IIB supergravity in $AdS_5 \times S^5$ and deforming it by turning on global charge density. The simplest setup — a truncation to Einstein-Maxwell theory — gives rise to the extremal RN-AdS black hole at vanishing temperature; fermion correlators in this background exhibit poles which can be associated with (non)Fermi liquid behavior [2-4].

The AdS_2 near-horizon geometry of the extremal RN-AdS black hole is the bulk feature responsible for this exotic behavior. However, the generic extremal black hole also has a finite entropy density at zero temperature signalling that the groundstate is unstable. It is natural to ask whether there are finite density states, preserving the AdS_2 factor, that do have vanishing entropy at zero temperature. The answer is affirmative; turning on two out of three diagonal $U(1)$ global charges in the IIB $AdS_5 \times S^5$ supergravity gives rise to a special class of charged dilatonic black holes studied in [5-6] (see also [7] for recent developments). The ten-dimensional string metric is known and can be dimensionally reduced down to five dimensions. The resulting near-horizon geometry is conformal to $AdS_2 \times R^3$, but the conformal factor ensures that the entropy at small temperatures vanishes linearly, $S \sim T$.

As shown in [6], fermion correlators in this background can be computed analytically and exhibit the sought-for (non-)Fermi liquid behavior, but now in an entropically stable system. In addition the system may carry additional fermionic excitations “behind the horizon” [8]. A potential probe of the presence of these “hidden” Fermi surfaces is the entanglement entropy (EE). As discussed in [9-12], in $d+1$ dimensional theory entanglement entropy of a ball of radius R in the presence of the Fermi surface behaves like $S_{ball,FS} \sim R^{d-1} \log R$, which violates the naive area law, $S_{ball} \sim R^{d-1}$. In general, computing entanglement entropy in the interacting field theories is a very nontrivial exercise. Fortunately, in the context of holographic duality, a simple prescription has been formulated by Ryu and Takayanagi [13-14]. Recent work on holographic matter with hyperscaling violation [8] (following [15]; see also [16-25] for subsequent work on holographic entanglement in the presence of hyperscaling violation) identified a set of examples, labeled

by the dynamical critical exponent z , which exhibit such logarithmic violation. All these examples involve the hyperscaling violation parameter set to be $\theta = d - 1$ and feature the low temperature behavior of the thermal entropy $S \sim T^{(d-\theta)/z} \sim T^{1/z}$.

It has been pointed out in [26] that in order for models with generic values of z and θ to holographically describe Fermi liquids, one should take the limit $z \rightarrow \infty$, $\theta \rightarrow -\infty$ with the limit θ/z held fixed. This is necessary in order to have a finite spectral density at finite values of momenta. Interestingly, the entropically stable charged dilatonic black holes studied in [6] precisely fall in this class. As we have already remarked, it also exhibits specific heat which vanishes linearly in temperature. As pointed out in [26], the simplest computation of entanglement of a belt in this geometry involves a phase transition and the resulting hypersurface in the bulk becomes disjoint when the belt becomes sufficiently thick. The latter phase of course signals the simple area law for the entanglement entropy.

In this paper we compute the entanglement entropy of a ball, and observe that contrary to the slab case, there is no phase transition to the disjoint configuration. However, the numerical results indicate that in the limit of a large size, the entanglement entropy of a ball still exhibits the area law. The explicit absence of a phase transition for ball-entanglement-entropy is odd compared to the belt configuration. One may think of the belt as the limit of two concentric balls with large radii but fixed difference. Geometrically, the belt phase transition is then of the Gross-Ooguri type for concentric Wilson loops [27-32]. When the difference between the radii is small, the minimal embedding surface is a half-torus; when the difference is large, the minimal embedding is two concentric spheres.

We also investigate entanglement entropy in the presence of higher derivative (Gauss-Bonnet) term in the gravity action to address how general these results are. The prescription for computing entanglement entropy in the presence of such a term has been formulated in [33-35], and we assume that it is not modified in the presence of additional matter in the bulk. In the holographic Gauss-Bonnet gravity we restrict our attention to the EE of a slab in the geometry with hyperscaling violation (which described the near horizon region the the Einstein-Hilbert case). Already here we encounter a surprise: the connected entangling surface does not end on the boundary for large values of the thickness ℓ of the slab; it can instead approximate the boundary but never get there. We expect that completing the geometry would lead to the same picture as that for the ball entanglement entropy in the Einstein-Hilbert case: no phase transition and a connected surface in the bulk defined for all large values of ℓ .

The paper is organized as follows. In the next Section we review both the 5-dimensional dilatonic black hole and its 10-dimensional lift and show that entanglement entropy calculation is equivalent in both settings. In Section 3 we compute entanglement entropy of simple geometries and observe that the calculations in the case of a belt and in the case of a ball are very different. In the former case there is a maximal value of the belt thickness, which can support a curved entangling surface; beyond that value there is a phase transition to a disjointed entangling surface. In the case of a ball, the entangling surface in the bulk stays connected and arbitrary large values of the ball radius R are supported. However, the entanglement entropy exhibits an area law in both cases. In Section 4 we study EE in the case of Gauss-Bonnet gravity and comment on the differences with the Einstein-Hilbert case. We discuss our results in Section 5. In the appendix we present some details of EE in Gauss-Bonnet gravity computed in the holographic duals of states with hyperscaling violation.

Note Added: When this paper was completed [36] appeared where the entanglement entropy of a straight belt in the five-dimensional black hole geometry was computed. This partially overlaps with Section 3.

2. Entanglement entropy and dimensional reduction

As pointed out in the introduction, one of the characteristic properties of systems with a Fermi surface, is the logarithmic violation of the area law of entanglement entropy [9-12]. Such logarithmic violations were recently found [8-16] in a class of holographic, albeit singular (with exception the case $\theta > 0$ and $z = 1 + \frac{\theta}{d}$ in $d + 2$ bulk spacetime dimensions¹), geometries with flux. It was subsequently realized that these class of geometries additionally exhibit other characteristic properties of Fermi surfaces, such as the scaling of the entropy with temperature at low temperatures, *i.e.*, $S \sim T^{\frac{1}{z}}$ [8].

The geometries in question are characterized by a critical exponent z and a hyperscaling violation exponent θ and are described by

$$ds^2 = \frac{1}{r^2} \left(-\frac{dt^2}{r^{2d(z-1)/(d-\theta)}} + g_0 r^{\frac{2\theta}{(d-\theta)}} dr^2 + \sum_{i=1}^d dx^2 \right), \quad (2.1)$$

¹ We thank Edgar Shaghoulian for correcting a mistake in this statement in the earlier version of the article.

where the UV boundary is located at $r = 0$ and the IR corresponds to large values of r . They can be found as solutions of the field equations emanating from

$$\mathcal{L} = R - Z(\Phi)F^2 - (\partial\Phi)^2 - V(\Phi) \quad (2.2)$$

where the dilatonic scalar field Φ and the Maxwell field A are additionally turned on. The parameter g_0 which appears in (2.1) is related to the IR behavior of the potential $V(\Phi)$.

This class of models has been extensively discussed in [37-41]. The logarithmic violation of the area law in entanglement entropy is realized for $\theta = d - 1$. Scale transformations act on these geometries [8]

$$\begin{aligned} \vec{x} &\rightarrow \Lambda \vec{x} \\ t &\rightarrow \Lambda^z t \\ ds &\rightarrow \Lambda^{\frac{\theta}{d}} ds \\ r &\rightarrow \Lambda^{\frac{(d-\theta)}{d}} r \end{aligned} \quad (2.3)$$

and lead to the following behavior for the thermal entropy $S \sim T^{\frac{(d-\theta)}{z}}$, explicitly verified in [15] and [8]. One recognizes how the hyperscaling violation exponent *theta* parametrizes the effective dimensional reduction.

An interesting special case of (2.1) involves the double scaling limit

$$z \rightarrow \infty \quad -\frac{\theta}{z} \equiv \eta > 0, \quad (2.4)$$

with η fixed. As emphasized in [26] several physical quantities behave as expected for Fermi liquids in this limit. The spacetime metric becomes conformal to $AdS_2 \times R^d$

$$ds^2 = \frac{1}{r^2} \left(-\frac{dt^2}{r^{\frac{2d}{\eta}}} + g_0 \frac{dr^2}{r^2} + \sum_{i=1}^d dx_i^2 \right), \quad (2.5)$$

while the thermal entropy vanishes like $S \sim T^\eta$ for small temperatures. More importantly the spectral density remains finite at low energies and finite momenta [26].

Here we are interested in a specific example of (2.5), the dilatonic black hole in AdS_5 recently explored in [5-6]. This black hole is usually referred to as the two-charge black hole, because it arises as a truncation of IIB supergravity on $AdS_5 \times S^5$ where two of the three $U(1)$ charges are equal and non-vanishing while the third one is zero [42].

After this truncation one obtains the Lagrangian

$$\mathcal{L} = R - \frac{1}{4} e^{4\alpha} F_{\mu\nu}^2 - 12 (\partial_\mu \alpha)^2 + \frac{1}{L^2} (8e^{2\alpha} + 4e^{-4\alpha}) \quad (2.6)$$

with α a scalar field and $F_{\mu\nu}$ the field strength of the Maxwell field A_μ . The extremal black hole metric

$$ds^2 = e^{2A} (-h dt^2 + dx^2) + \frac{e^{2B}}{h} dr^2 \quad (2.7)$$

with

$$\begin{aligned} A &= \ln \frac{r}{L} + \frac{1}{3} \ln \left(1 + \frac{Q^2}{r^2} \right), \\ B &= -\ln \frac{r}{L} - \frac{2}{3} \ln \left(1 + \frac{Q^2}{r^2} \right) \\ h &= \frac{(r^2 + 2Q^2)r^2}{(r^2 + Q^2)^2} \end{aligned} \quad (2.8)$$

together with

$$A_\mu dx^\mu = \frac{\sqrt{2}Qr^2}{L(r^2 + Q^2)} dt, \quad \alpha = \frac{1}{6} \ln \left(1 + \frac{Q^2}{r^2} \right) \quad (2.9)$$

form a solution of the equations of motion coming from (2.6). In these coordinates, large r corresponds to the near-boundary UV region while the black hole horizon is located at $r = 0$. To be precise, $r = 0$ is actually a naked singularity. Any finite temperature will cloak the singularity, however, so it is of the “good” type. In the near-horizon region, (2.7) is conformal to $AdS_2 \times R^3$ [6]

$$ds^2 = \left(\frac{r}{Q} \right)^{\frac{2}{3}} \left(-\frac{2r^2}{L^2} dt^2 + \frac{L^2}{2r^2} dr^2 + \frac{Q^2}{L^2} \sum_{i=1}^3 dx_i^2 \right). \quad (2.10)$$

With a change of variable from r to \tilde{r} such that $\frac{r}{Q} = \frac{1}{\sqrt{2}\tilde{r}^3}$ the IR metric reduces to

$$ds^2 = \frac{1}{\tilde{r}^2} \frac{Q^2}{2^{\frac{1}{3}} L^2} \left(-\frac{dt^2}{\tilde{r}^6} + \frac{9L^4}{2Q^2} \frac{d\tilde{r}^2}{\tilde{r}^2} + \sum_{i=1}^3 dx_i^2 \right). \quad (2.11)$$

Thus (2.11) is of the form (2.5) with $g_0 = \frac{9L^4}{2Q^2}$ and $\eta = 1$.

By the definition of consistent truncation, this solution can be lifted to a solution of the full IIB supergravity with $Q_1 = Q_2 = Q$ and $Q_3 = 0$ [42]. This ten dimensional solution is

$$\begin{aligned} ds^2 &= \sqrt{\Delta} H^{-\frac{2}{3}} \left[e^{2A} \left(-h dt^2 + \sum_{i=1}^3 dx_i^2 \right) + \frac{e^{2B}}{h} dr^2 \right] \\ &+ \frac{L^2 H}{\sqrt{\Delta}} \sum_{i=1}^2 \left[d\mu_i^2 + \mu_i^2 \left(d\phi_i + \frac{Q}{L^2 H} (1 - H) dt \right)^2 \right] + \frac{L^2}{\sqrt{\Delta}} (\cos^2 \theta_1 d\theta_1^2 + \sin^2 \theta_1 d\phi_3^2) \\ F_5 &= G_5 + \star G_5 \quad G_5 = dB_4 \quad B_4 = -\frac{r^4}{L^4} \Delta dt \wedge d^3 x - \frac{Q^3}{L^2} \sum_{i=1}^2 \mu_i^2 d\phi_i \wedge d^3 x. \end{aligned} \quad (2.12)$$

where

$$H = 1 + \frac{Q^2}{r^2}, \quad \Delta = H(\cos^2 \theta_1 + H \sin^2 \theta_1) \quad (2.13)$$

and h, A, B are given in (2.8). Here μ_1 and μ_2 are defined as

$$\mu_1 \equiv \cos \theta_1 \cos \theta_2, \quad \mu_2 \equiv \cos \theta_1 \sin \theta_2. \quad (2.14)$$

where θ_1, θ_2 are coordinates on the S^2 inside the S^5 which is parametrized by $(\theta_1, \theta_2, \phi_1, \phi_2, \phi_3)$. The solution describes N coincident $D3$ branes, rotating with equal angular momentum in the two out of the three possible planes of rotation transverse to the $D3$ -brane world-volume.

As explained in the introduction, our main focus will be on entanglement entropy. A natural question to ask is whether the computation of entanglement entropy in the ten dimensional geometry (2.12) is equivalent with the one in five dimensions. In the simple case of p-branes, [43] and [17] showed that the two computations, in the ten dimensional setup and in the dimensionally reduced geometry, agreed as long as the former was done in string frame and the latter in the Einstein frame. In what follows, we will show that this is also true for (2.12) and (2.7).

Let us consider the entanglement entropy of some arbitrary connected region and parametrize the entangling surface by a single function $r(x_1, x_2, x_3)$. The induced metric for a surface in the geometry of (2.12) which asymptotes to the entangling surface under consideration is

$$\begin{aligned} ds_{EE}^2 = & \sqrt{\Delta} H^{-\frac{2}{3}} e^{2A} \left[\delta_{ij} + \frac{e^{2B-2A}}{h} (\partial_i r)(\partial_j r) \right] dx^i dx^j + \\ & + \frac{L^2}{\sqrt{\Delta}} [H c_1^2 d\theta_2^2 + H c_1^2 (c_2^2 d\phi_1^2 + s_2^2 d\phi_2^2) + s_1^2 d\phi_3^2] + \frac{L^2 \sqrt{\Delta}}{H} d\theta_1^2 \end{aligned} \quad (2.15)$$

where we introduced the notation $c_i = \cos \theta_i$, $s_i = \sin \theta_i$ and used the definition of Δ in (2.13) to simplify the expression. The entropy functional is proportional to the volume of the induced metric, which integrated over the five dimensional compact space yields

$$\sqrt{g_{EE}} = Vol_5 e^{3A} \sqrt{\det \left[\delta_{ij} + \frac{e^{2B-2A}}{h} (\partial_i r)(\partial_j r) \right]}. \quad (2.16)$$

where $Vol_5 = L^5 \Omega_5$ is the volume of the five dimensional sphere of radius L . Finally, the entanglement entropy computed with the ten-dimensional metric (2.12) is given by

$$S_{slab}^{EE} = \frac{1}{G_N^5} \int d^3 x e^{3A} \sqrt{\det \left[\delta_{ij} + \partial_i r \partial_j r \frac{e^{2B-2A}}{h} \right]} \quad (2.17)$$

where we used the relation $\frac{1}{G_N^5} = \frac{Vol_5}{G_N^{10}}$. As expected, (2.17) precisely coincides with the entropy functional computed in the dimensionally reduced metric (2.7). Note that in the ten-dimensional metric the singularity is that of a conventional rotating black brane. The equivalence thus guarantees that the apparent naked singularity in the five-dimensional extremal black hole metric (2.7) is innocuous and does not affect the results.

In summary, computing entanglement entropy in the ten-dimensional geometry is completely equivalent to computing it in the five dimensional geometry.

3. Entanglement entropy for the dilatonic black hole

In this Section we will compute holographic entanglement entropy in the theory described by the metric (2.7). In the following we set $L = 1$. It will be useful to write the near-horizon limit of the metric (2.7) in the following form

$$ds^2 = 2^{-\frac{5}{3}} Q^{-\frac{2}{3}} z^{-\frac{2}{3}} \left(\frac{-dt^2 + dz^2}{z^2} + \sum_{\mu=1}^3 d\tilde{x}_\mu^2 \right) \quad (3.1)$$

where $\tilde{x}_\mu = \sqrt{2}Qx_\mu$ and $z = 1/2r$. Note that the metric (3.1) belongs to the class of metrics studied in [8] with a particular value of dynamical exponent $z = \infty$. We start by placing a system in the large 3-dimensional box of size L_x , which serves as an IR regulator. We can now compute the entanglement entropy of a slab, specified by $0 \leq x_1 \leq \ell$, $0 \leq x_2, x_3 \leq L_x$, where $\ell \ll L_x$. The entangling surface can be parameterized by a single function $x_1(z)$ with the boundary conditions $x_1(0) = 0, \ell$. The entropy functional takes the form

$$S_{slab} = L_x^2 \int \frac{dz}{z} \sqrt{\frac{1}{z^2} + (x')^2} \quad (3.2)$$

where $x \equiv \sqrt{2}Qx_1$, the prime denotes derivative with respect to z and the integral needs to be appropriately regularized. In (3.2) and in the rest of the paper we omit an overall numerical factor, together with a factor of L^2/ℓ_p^2 , which roughly measures the number of degrees of freedom (in the case of the holographic dual of a conformal field theory such a factor is proportional to the central charge). The equation of motion that results from (3.2) can be written as

$$\frac{x'}{z\sqrt{z^{-2} + (x')^2}} = \frac{1}{z_0} \quad (3.3)$$

where $1/z_0$ is a constant of motion; the value of $z = z_0$ corresponds to the turning point of the curve in the bulk where $x' = \infty$. By varying the value of z_0 one can change the shape of the curve. The value of ℓ as a function of z_0 can be computed via

$$\sqrt{2}Q\ell = 2 \int dz x' = 2 \int_0^{z_0} \frac{dz}{z} \frac{1}{\sqrt{(z_0/z)^2 - 1}} = \pi. \quad (3.4)$$

The key feature of this result is its independence of the value of z_0 : the curved hypersurface in the bulk which approximates to the boundaries of the slab on the AdS boundary can only do so for a fixed thickness of the slab ℓ . We are, of course, interested in the behavior of the EE as ℓ is taken to be large. At this point it is worth recalling that there is always a trivial solution $x' = 0$: this becomes the only available solution for $Q\ell \neq \pi/\sqrt{2}$. It is clear that the entanglement entropy for such a solution is independent of ℓ . (this feature of the geometry (2.7) has been pointed out before; see e.g. [26].)

When the full geometry (2.7) is considered, we might expect the picture to be the following. For sufficiently large ℓ the hypersurface in the bulk should probe the infrared limit of the geometry (2.7), described by (3.1). Therefore the discussion of the previous paragraph applies: there is a maximal value of $\ell = \ell_{crit}$ which corresponds to the curved solution; beyond it only the trivial $x' = 0$ solution exists. The transition between the two configurations is second order, since the curved solution asymptotically approaches the trivial one as $\ell \rightarrow \ell_{crit}$. For sufficiently small ℓ the entangling surface probes the UV (small z region) of the geometry, and we expect ℓ to be a smooth function of z_0 with a limit $\ell(z_0 = 0) = 0$. To check these expectations we repeat the calculation above for the full geometry (2.7). The EE functional is now given by

$$S_{slab} = L_x^2 \int dz e^{2A} \sqrt{e^{2B}/h + e^{2A}(x')^2} \quad (3.5)$$

The analog of (3.4) is now given by

$$Q\ell = 2 \int_{\tau_0}^{\infty} \frac{d\tau}{\sqrt{\tau^2(2 + \tau^2) (\tau^2(1 + \tau^2)^2 \tau_0^{-2} (1 + \tau_0^2)^{-2} - 1)}} \quad (3.6)$$

where $\tau = r/Q$, $\tau_0 = r_0/Q$. The value of this integral as a function of τ_0 is plotted in Fig. 1.

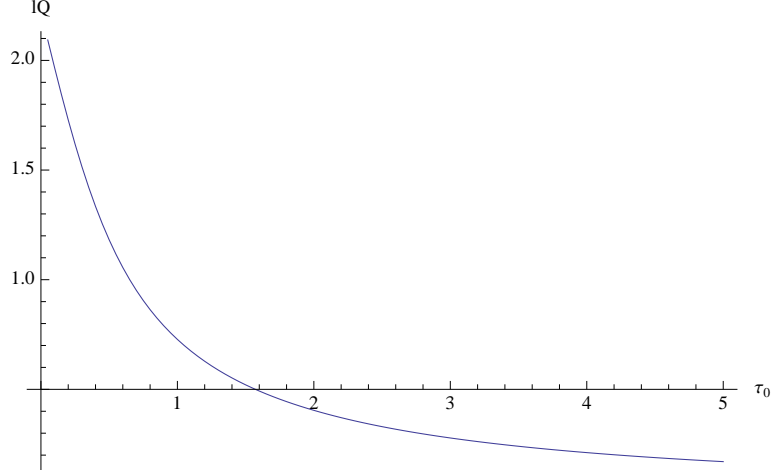


Fig. 1: ℓQ as a function of τ_0 computed using eq. (3.6).

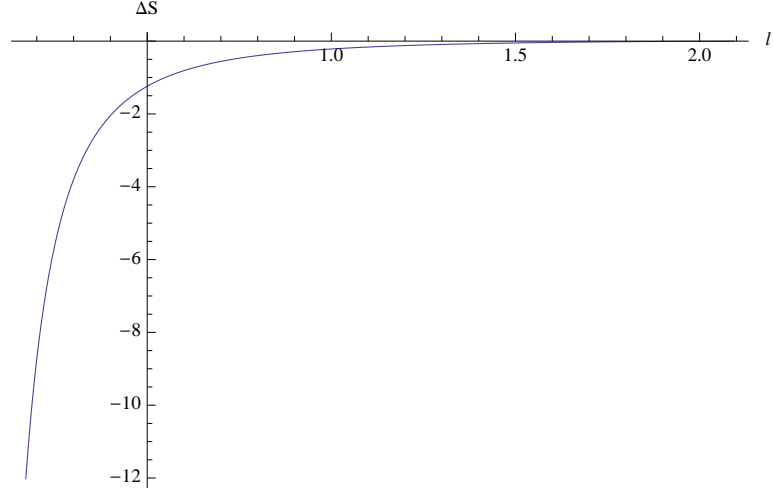


Fig. 2: ΔS as a function of ℓQ .

The figure is in accord with the general discussion above. In the UV region, $\tau_0 \gg 1$, the length of the interval monotonically decreases to zero. On the other hand, there is a limiting value of ℓ as the position of the tip approaches the horizon at $\tau = 0$. Note that this limiting value is equal to $\ell_{crit} = \pi/\sqrt{2}Q$, in accord with the near-horizon analysis. We check that for $\ell \leq \ell_{crit}$ the curved solution is preferred (gives the leading contribution to the EE), and the difference vanishes in the limit $\ell \rightarrow \ell_{crit}$. (see Fig. 2).

The next step is computing the entanglement entropy for a sphere, defined by

$$\sum_{\mu=1}^3 x_{\mu}^2 = \frac{\rho^2}{2Q^2} \leq R^2 \quad (3.7)$$

We start by considering the near-horizon metric (3.1). The entangling surface in the bulk can be parameterized by a single function $z(\rho)$; the EE functional is given by

$$S_{sphere} = \int \frac{d\rho}{z} \rho^2 \sqrt{(z')^2/z^2 + 1}. \quad (3.8)$$

The equation of motion is now second order:

$$\frac{\partial}{\partial \rho} \left(\frac{\rho^2 z'}{z^3 \sqrt{(z')^2/z^2 + 1}} \right) = - \frac{\rho^2 (z^2 + 2(z')^2)}{z^4 \sqrt{(z')^2/z^2 + 1}} \quad (3.9)$$

We can integrate this numerically; the result is given by the red curve in Fig. 3. The surprising feature of eq. (3.9) is the absence of the solutions approaching the boundary at $z = 0$ at finite ρ . Such a behavior has not been observed in the examples studied in [8]. This behavior is evident in Fig. 3. (the red curve never intersects the $z = 0$ line). Also, unlike the slab case, there are no trivial solutions $\rho(z) = \text{const.}$

The near-horizon approximation is clearly not reliable and we must we analyze the EE of a sphere in the full diatonic black hole metric (2.7). The EE functional now takes the form

$$S_{sphere} = \int \frac{d\rho}{z} \rho^2 e^{2A(z)} \sqrt{e^{2A(z)} + \frac{e^{2B(z)}(z')^2}{4z^4 h(z)}} \quad (3.10)$$

where $A(z), B(z), h(z)$ are determined by (2.8) with the substitution $z = 1/2r$. The equation of motion for $z(\rho)$ that follows from (3.10) is second order and has to be dealt with numerically. A representative solution is shown in Fig 3 (blue curve). The red curve corresponds to the solution in the near horizon geometry. The modification of the EOM in the full geometry ensures that the hypersurface now reaches the boundary at finite ρ .

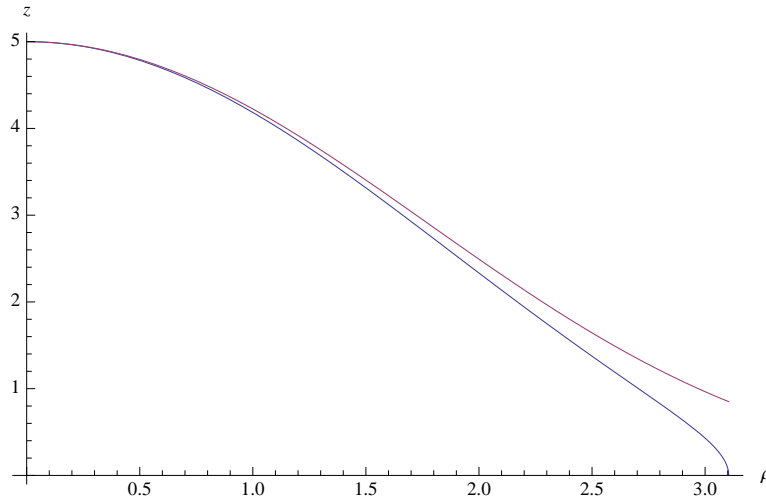


Fig. 3: $z(\rho)$ for the near horizon (red) and full BH metric (blue)

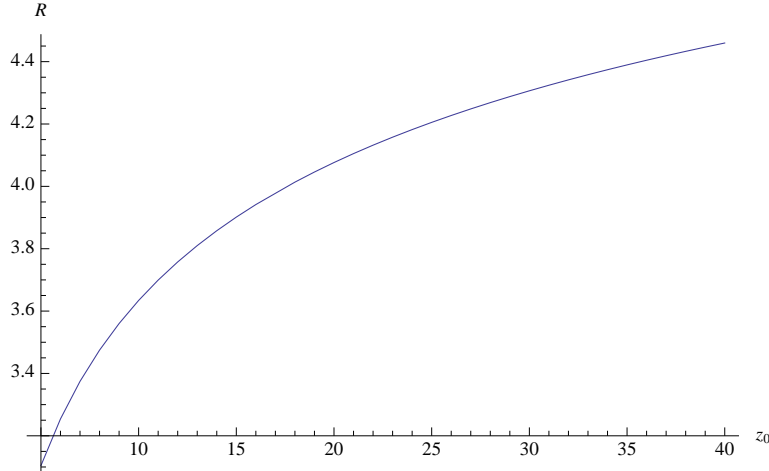


Fig. 4: R as a function of z_0 for the full BH metric

We can now compute the radius of the entangling surface at the boundary as a function of z_0 numerically. The result is shown on Fig 4. Finally we are in position to compute the value of entanglement entropy. (Similar computations have recently appeared in [44] and [45]; we will follow the procedure outlined in [32], which the reader is encouraged to consult for technical details.) The entanglement entropy of a ball is UV divergent and a suitable regularization is necessary. The UV divergent terms are governed by the asymptotically AdS_5 metric; these terms in the conformal case have been computed in [14]:

$$S_{ball,divergent} = \frac{R^2}{8\epsilon^2} + \frac{1}{2} \log \epsilon \quad (3.11)$$

here $\epsilon \ll 1$ is the cutoff on the radial coordinate z . An extra factor of $1/2$ in the first term in (3.11) compared to eq. (7.10) in [14] appears due to the factor of two in the definition of z in our paper.

All we need is to evaluate (3.10) on the solution of equation of motion, and subtract the UV divergent term (3.11). We are interested in the deviation of the resulting finite quantity, $S_{UV\,finite} = S_{ball} - S_{ball,divergent}$ from the area law. In Fig. 5 we plot the normalized UV finite part of the entanglement entropy. One observes directly that at large R the behavior of entanglement entropy of a ball is governed by the area law. The equation of motion does not appear to have a second distinct class of solutions and the result implies that the ball-entanglement entropy does not experience a phase transition at smaller radius to a phase differing from the naive area law.

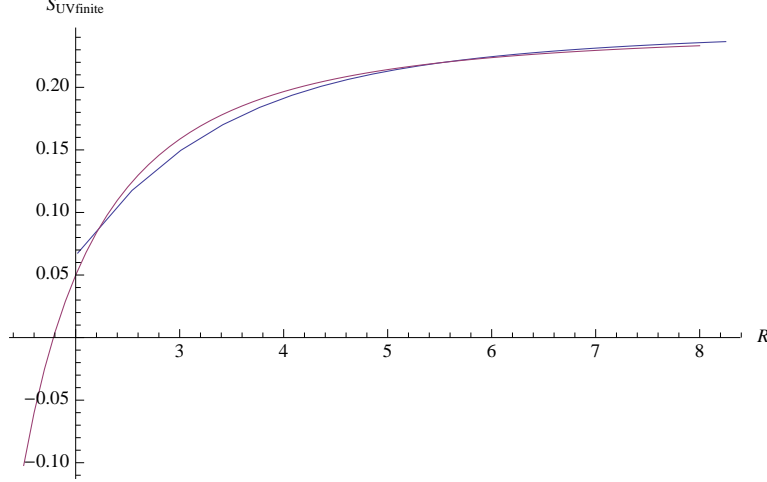


Fig. 5: $S_{UV\,finite}/R^2$ as a function of RQ ; red curve corresponds to $S_{UV\,finite}/Q^2 R^2 = 0.25 - 0.78/Q^2 R^2$ fit.

4. Gauss-Bonnet and the EE of a belt

Here we compute the entanglement entropy of a belt in Gauss-Bonnet gravity. We use the near horizon geometry of eqs. (3.1) which is a solution to the equations of motion following from dilatonic Gauss Bonnet gravity with flux (see the appendix for more details). Entanglement entropy in Gauss-Bonnet gravity is given by extremizing the action functional [34-35]

$$S = \int d^3x \sqrt{\det G_\Sigma} (1 + \lambda R_\Sigma) \quad (4.1)$$

where λ is the Gauss-Bonnet coupling constant whereas G_Σ and R_Σ refer to the induced metric and the induced scalar curvature ².

Consider the slab, specified by $0 \leq x_1 \leq \ell$ and $x_2, x_3 \leq L_x$ with $L_x \gg \ell$ as in section 3. The entangling surface is parametrized by a single function $x_1(z)$ and gives rise to the induced geometry

$$ds^2 = 2^{-\frac{5}{3}} Q^{-\frac{2}{3}} z^{\frac{2}{3}} \left[\left(\frac{1}{z^2} + \dot{x}_1^2(z) \right) dz^2 + \sum_{i=2}^3 d\tilde{x}_i^2 \right], \quad (4.2)$$

where the dot implies differentiation with respect to the variable z and $\tilde{x}_i = \sqrt{2}Qx_i$. The action functional (4.1) reduces in this case to

$$S_{slab} = 2^{-5} Q^{-2} L_x^2 \int \frac{dz}{z} \sqrt{\frac{1}{z^2} + \dot{x}^2} \left(1 - \frac{2\lambda z^{\frac{2}{3}} (1 + 7z^2 \dot{x}^2 + 6z^3 \dot{x}\ddot{x})}{9(1 + z^2 \dot{x}^2)^2} \right), \quad (4.3)$$

² To make the variational problem well-defined a boundary term should be added to (4.1). This term only affects the leading (proportional to λ) divergent term in the entanglement entropy, e.g. see [35], it will therefore not affect the results of this section.

where we set $x \equiv \sqrt{2}Q\tilde{x}_1$. The equation of motion following from (4.3) takes the form

$$\frac{\dot{x}}{\sqrt{1+z^2\dot{x}^2}} - \frac{2}{9}\lambda z^{\frac{2}{3}} \frac{\dot{x}}{(1+z^2\dot{x}^2)^{\frac{3}{2}}} = \frac{1}{z_0} \quad (4.4)$$

where z_0 is a constant of motion related to the width of the slab $\ell \equiv \frac{\tilde{\ell}}{\sqrt{2}Q}$ through

$$\frac{\tilde{\ell}}{2} = \int_{z_0}^0 dz \dot{x} \quad (4.5)$$

It is convenient to define a dimensionless variable $y = \frac{z}{z_0}$ which takes values in $y \in [0, 1]$ and express (4.4) as follows

$$\frac{x'}{\sqrt{1+y^2x'^2}} - \frac{2}{9}\lambda z_0^{\frac{2}{3}} \frac{x'}{(1+y^2x'^2)^{\frac{3}{2}}} - 1 = 0, \quad (4.6)$$

where now primes indicate differentiation with respect to the new variable y . Eq. (4.6) shows that the presence of the Gauss-Bonnet coupling strongly affects the physics of the entanglement entropy. In particular, $x'(y)$ now depends on z_0 through $B \equiv \lambda z_0^{\frac{2}{3}}$. As a result the length of the slab $\tilde{\ell}$, which in y coordinate is given by

$$\frac{\tilde{\ell}}{2} = \int_0^1 dy x'(y), \quad (4.7)$$

is not anymore independent of z_0 . Note that we have taken $z_0 \geq 0$ to make contact with the $\lambda = 0$ limit.

To proceed we need to solve (4.6) for $x'(y)$. Obviously, the disconnected solution, $x' = 0$ is always a solution. There also exist three connected solutions to (4.6) but, as commonly observed in Gauss-Bonnet gravity, only one of them asymptotes to the connected solution when λ vanishes³. We choose this solution for x' and proceed to examine its behavior close to the boundary $y = 0$. We find that for all $B \geq \frac{9}{2}$ $x'(y)$ diverges as y approaches the boundary

$$x' = \begin{cases} \frac{\sqrt{-9+2B}}{2y} + \frac{\sqrt{2}B^{3/2}}{-27+6B} + \mathcal{O}(y) & B > \frac{9}{2} \\ \frac{1}{y^{\frac{2}{3}}} + \frac{1}{2} + \frac{3y^{\frac{2}{3}}}{8} + \mathcal{O}(y^{\frac{4}{3}}) & B = \frac{9}{2} \end{cases} \quad (4.8)$$

³ It would be interesting to study all possible solutions in detail in the spirit e.g. of [46].

whereas it goes to a constant for $B < \frac{9}{2}$

$$x' = \frac{9}{9-2B} + \frac{9}{2} 3^{\frac{1}{3}} \frac{-3+2B}{(-9+2B)^4} y^2 + \mathcal{O}(y^4) \quad B < \frac{9}{2} \quad (4.9)$$

Hence, a solution which asymptotes to the entangling surface only exists for $B < \frac{9}{2}$. A natural question to ask is whether this result changes when one considers the full solution and not just the near horizon geometry. We leave this to future investigation.

It is instructive to also consider the behavior of the solution close to the turning point $y = 1$. One essentially finds that the solution becomes complex for $B < -\frac{9}{4}$, in other words it ceases to exist. For $B > -9/4$ x' diverges at $y \sim 1$ and the solution tends to a constant value. We will therefore restrict to values of B lying in the region $-\frac{9}{4} \leq B < \frac{9}{2}$.

Substituting this solution into (4.7) and performing the integration numerically shows that for $B \in (-\frac{9}{4}, \frac{9}{2})$, the length of the slab $\tilde{\ell}$ varies from $\tilde{\ell} \in (0.4, 3\pi)$. However, since $z_0 \geq 0$, the sign of B is completely determined by the sign of the Gauss-Bonnet coupling λ which according to the null energy condition (see appendix) is bounded above by $\lambda \leq \frac{9}{2}$. This implies that both signs are allowed for B . It would be interesting to see if other constraints, such as those discussed in [47-50], can uniquely fix the sign of λ .

The length $\tilde{\ell}$ as a function of B for positive values of B is plotted in Fig. 6.

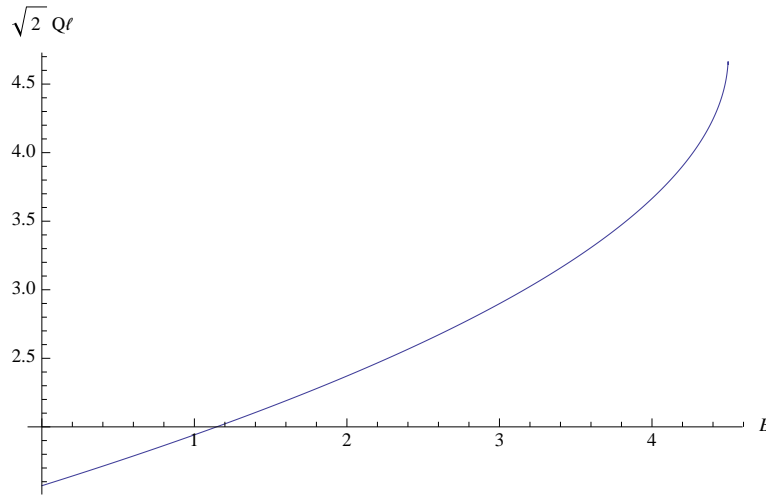


Fig. 6: $\tilde{\ell}$ as a function of $B \equiv \lambda z_0^{\frac{2}{3}}$ for $B \geq 0$. A solution only exists for $\tilde{\ell} < 3\pi$.

Fig. 7 instead shows $\tilde{\ell}$ for negative values of B . The two curves join at the point $B = 0$ where the result of section 3 is recovered; the connected solution exists only for $\tilde{\ell} = \pi$.

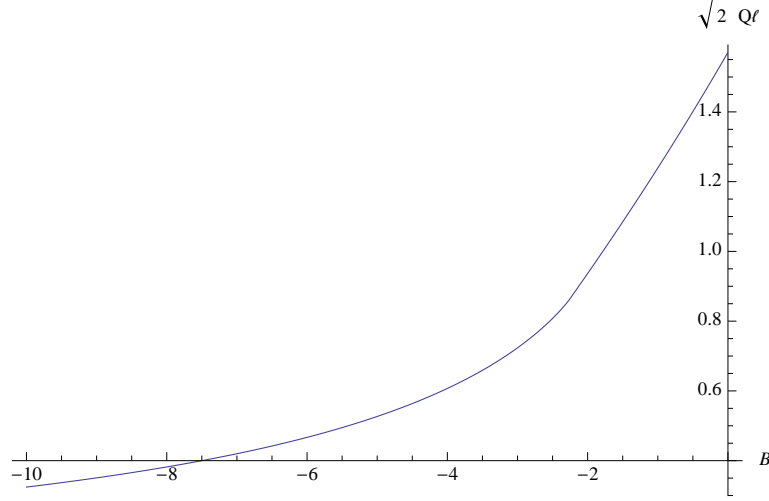


Fig. 7: $\tilde{\ell}$ as a function of $B \equiv \lambda z_0^{\frac{2}{3}}$ for $\lambda \leq 0$.

In summary, for negative λ the connected solution exists for $\tilde{\ell} \in [0.4, \pi)$ whereas for non-negative λ , it exists for $\tilde{\ell} \in [\pi, 3\pi)$.

We conclude this section by computing the difference between the entanglement entropy of the connected solution and the disconnected one. The difference is given by⁴

$$\begin{aligned} \frac{32Q^2}{L_x^2} \Delta S_{belt} &\equiv \frac{32Q^2}{L_x^2} (S_{belt, con.} - S_{belt, disc.}) = \\ &= \left(\frac{\lambda}{B} \right)^{\frac{3}{2}} \left\{ \left(-1 + \frac{2B}{3} \right) + \right. \\ &\quad \left. + \int_0^1 dy \left(\frac{\left(9 - 2By^{\frac{2}{3}} \right)^2 - 54 \left(-3 + 2By^{\frac{2}{3}} \right) y^2 x'^2 - 9 \left(-9 + 8By^{\frac{2}{3}} \right) y^4 x'^4}{9y^2 \sqrt{1 + y^2 x'^2} \left(9 - 2By^{\frac{2}{3}} + \left(9 + 4By^{\frac{2}{3}} \right) y^2 x'^2 \right)} - \frac{-9 + 2By^{\frac{2}{3}}}{9y^2} \right) \right\} \end{aligned} \quad (4.10)$$

where we used (4.6) and the fact the (4.3) is independent of x , to express the integral in terms of x' alone. In Fig. 8 we plot ΔS for positive B and in Fig. 9 for negative B .

It is easy to see that for positive Gauss-Bonnet coupling, the connected solution—whenever available—is favoured, while the contrary happens for negative values of the coupling.

5. Discussions and puzzles

In this paper we computed holographic entanglement entropy in the background which corresponds to the finite density state in the $\mathcal{N} = 4$ SYM theory with two equal $U(1)$

⁴ In the following we express the difference in the entropy in terms of B instead of ℓ for reasons of convenience. Note that B is a monotonic function of ℓ .

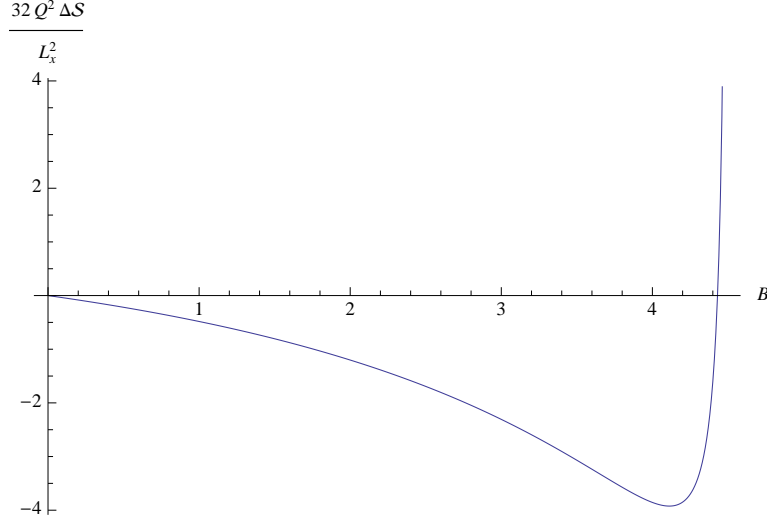


Fig. 8: ΔS as a function of B for $B \geq 0$.

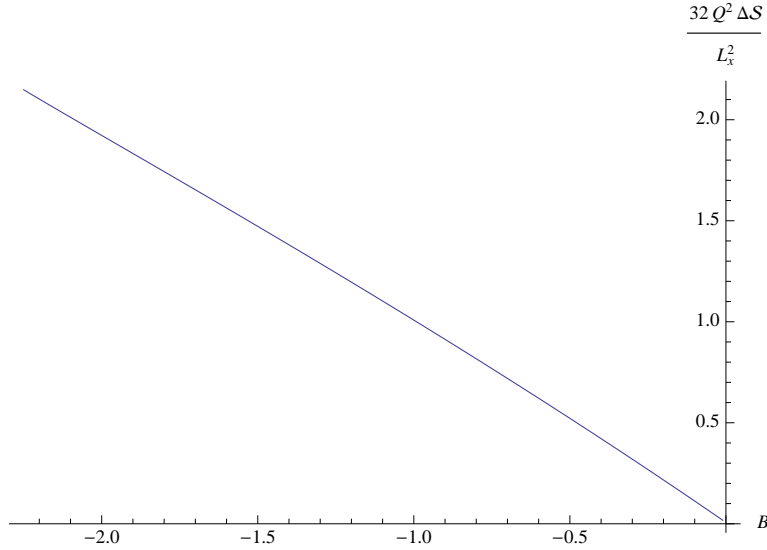


Fig. 9: ΔS as a function of B for $B < 0$.

charges. The computations were done for two simple geometries: a belt and a sphere. The puzzle we encounter is that we observed a phase transition in the case of a belt as a function of its width, whereas the sphere does not.

Such phase transitions in entanglement entropies have been observed before in confining geometries [51][43][32]. (Of course, to make intelligent statements about the phase transitions, one needs to define a UV-finite quantity; one suitable definition in our case would involve subtracting the entanglement entropy in the vacuum, zero density state.) In [43] a field theoretic explanation of this effect was proposed: the value of entanglement for

the free glueball of mass m is exponentially suppressed, $S \sim \exp(-m\ell)$; integrating this over the glue ball density of states with Hagedorn behavior, $\rho(m) \sim \exp(\beta_H m)$ produces a phase transition at $\ell \sim \beta_H$. The transition, which resembles Hagedorn phase transition, is between the $\mathcal{O}(1)$ values of entanglement for sufficiently large values of ℓ and $\mathcal{O}(N^2)$ values for small values of ℓ , where the integral over glue ball states formally diverges.

One would argue that the phase transition is a universal phenomenon only depending on the size of the entangling surface compared to the density. Indeed in [32] a similar phase transition has been observed for the entanglement entropy of a sphere (disk) in confining geometries dual to the 3+1 (2+1) dimensional theories. This raises a second puzzle, since the (UV-finite part of) the free field entanglement entropy in this case is not exponentially suppressed, but rather has an expansion in the inverse powers of the radius (see e.g. [52-53]).

We do not have a resolution of this second puzzle. Nor do we have a fundamental answer to the first. Instead, we add the observation that an understanding of these phase transitions must be more complicated in that a third scale must play a role. This third scale is supplied by the anisotropy of the belt. This must be so as one ought to be able to obtain the belt shape by deforming the ball-entangling surface continuously into an ovoid. In this process the phase-transition should suddenly appear; qualitatively it must therefore depend on the eccentricity of the ovoid. To check this explicitly is technically quite involved. One can, however, easily construct a different geometric set-up which interpolates between the ball and the belt and thereby argue that this interpretation is correct. This set-up is the annulus or two concentric balls. In the limit where the inner radius vanishes one has the sphere, and in the double limit where both radii are large, but the difference stays small, one has the belt. It is well-known from the analogue study of holographic Wilson loops that this annulus system has a phase transition between a geometric embedding surface that is a half-torus for the belt-like configuration and two nested sphere-like embeddings for the ball-like configuration [27-31]. This suggests that the belt-like phase transition may be a consequence of the third scale introduced by the anisotropy violation. It would be interesting to construct a free-field model which would reproduce this behavior, although there is no guarantee such a free field description exists.

Note, that for the case of states with Fermi surfaces, one expects the two geometries to produce the same violation of the area law (and this is also the case in the holographic models of [8]). Of course, the area law is not violated in our case, so one can conclude that the ground state dual to the geometry explored here is different from a Fermi liquid.

We would finally like to note that the addition of the Gauss-Bonnet term to the bulk Lagrangian modifies the picture. In this case there are strong indications that the belt geometry can support connected surfaces for arbitrarily large values of the distance between the plates. Generally, adding higher derivative terms such as the Gauss-Bonnet term amounts to the inclusion of $1/g_{YM}^2 N$ and/or $1/N$ corrections in the dual field theory. It suggests then that the phase-transition is a strong coupling/large N phenomenon which would be hard to capture in any field theoretic approach. The Gauss-Bonnet term is very special and we should be careful to extrapolate generic lessons from it.

Acknowledgements: We would like to thank J. Jottar, I. Klebanov, D. Kutasov, Y. Liu, S. Sachdev, and J. Zaanen for useful discussions. M.K. and A.P. thank Aspen Center for Physics where part of this work was completed. This work was supported in part by the NSF grant No. 1066293, a VIDI grant from NWO and by the Dutch Foundation for Fundamental Research on Matter (FOM). The work of M.K. was partially supported by the ERC Advanced Grant "SyDuGraM", by IISN-Belgium (convention 4.4514.08) and by the "Communauté Française de Belgique" through the ARC program and the NSF grant No. 1066293.

Appendix A. Gauss-Bonnet, hyperscaling violation and entanglement entropy.

A.1. Solutions of GB gravity+matter which give rise to holographic hyperscaling violation.

Here we show that geometries with hyperscaling violation are solutions of Gauss-Bonnet gravity with matter and gauge fields. We consider the following five-dimensional action

$$I_G = \frac{1}{16\pi G_N} \int d^{4+1}x \sqrt{-g} \left[R + \frac{12}{L^2} + \frac{\lambda L^2}{2} (R_{\mu\nu\rho\sigma}^2 - 2R_{\mu\nu}^2 + R^2) - \mathcal{L}^m \right] \quad (\text{A.1})$$

where λ is the dimensionless Gauss-Bonnet coupling and \mathcal{L}^m is the matter Lagrangian

$$\mathcal{L}^m = Z(\Phi)F^2 + \frac{1}{2}(\partial\Phi)^2 + V(\Phi). \quad (\text{A.2})$$

Here $\mathcal{L}(F^2)$ is an arbitrary function of the quadratic gauge invariant $F^2 = F_{\mu\nu}F^{\mu\nu}$, with $F_{\mu\nu} = \partial_\mu A_\nu - \partial_\nu A_\mu$ the electromagnetic tensor field and A_μ the vector potential. Φ is a scalar field and $V(\Phi)$, $Z(\Phi)$ are arbitrary functions. The action I_G should in principle be supplemented with a boundary term to make the variational problem well-defined. For our purposes the detailed structure of the boundary term will not be necessary.

Varying the action with respect to the metric tensor $g_{\mu\nu}$ and the matter fields Φ, A_μ yields the following equations of motion

$$\begin{aligned} G_{\mu\nu} - \frac{6}{L^2}g_{\mu\nu} + \frac{\lambda L^2}{2}G_{\mu\nu}^{(2)} &= T_{\mu\nu}^m \\ \nabla_\nu Z(\Phi) (F^{\mu\nu}) &= 0 \\ \partial_\mu (\sqrt{-g}g^{\mu\nu}\partial_\nu\Phi) - \sqrt{-g} \left(\frac{\partial V}{\partial\Phi} + \frac{\partial Z}{\partial\Phi}F_{\mu\nu}^2 \right) &= 0, \end{aligned} \tag{A.3}$$

where $G_{\mu\nu} \equiv R_{\mu\nu} - \frac{1}{2}Rg_{\mu\nu}$ is the Einstein tensor, $T_{\mu\nu}^m$ is the energy momentum tensor for the matter fields and $G_{\mu\nu}^{(2)}$ is the second order Lovelock tensor

$$\begin{aligned} G_{\mu\nu}^{(2)} &= 2 \left(R_{\mu\rho\kappa\lambda}R_{\nu}^{\rho\kappa\lambda} - 2R_{\mu\rho\nu\kappa}R^{\rho\kappa} - 2R_{\mu\rho}R_{\nu}^{\kappa} + RR_{\mu\nu} \right) - \\ &\quad - \frac{1}{2} \left(R_{\kappa\lambda\rho\sigma}^2 - 2R_{\kappa\lambda}^2 + R^2 \right) g_{\mu\nu}. \end{aligned} \tag{A.4}$$

The matter energy momentum tensor has the form

$$T_{\mu\nu}^m = -\frac{1}{2}g_{\mu\nu}\mathcal{L}^m + 2(\partial_\mu\Phi)(\partial_\nu\Phi) + 2Z(\Phi)F_\mu^\rho F_{\nu\rho}. \tag{A.5}$$

We search for solutions of the form

$$\begin{aligned} ds^2 &= e^{2A(r)} \left(dr^2 - e^{2B(r)} dt^2 + dx_i^2 \right) \\ A_t &= A_t(r) \quad A_i = 0, \quad i = 1, 2, 3, \quad \Phi = \Phi(r). \end{aligned} \tag{A.6}$$

Substituting the ansatz (A.6) into the equations of motion (A.3) yields

$$\begin{aligned} T_t^{t,m} - T_i^{i,m} &= 2F_{tr}F^{tr}Z(\Phi) = -e^{-2A(r)} \left(3A'(r)B'(r) + B'(r)^2 + B''(r) \right) + \\ &\quad + 2\lambda L^2 e^{-4A(r)} A'(r) \left[B'(r) \left(A'(r)^2 + A'(r)B'(r) + 2A''(r) \right) + A'(r)B''(r) \right] \\ T_r^{r,m} - T_t^{t,m} &= e^{-2A(r)} (\partial_r\Phi)^2 = \\ &= 3e^{-2A(r)} \left(1 - 2\lambda L^2 e^{-2A(r)} A'(r)^2 \right) \left(A'(r)^2 + A'(r)B'(r) - A''(r) \right) \\ \partial_r \left(e^{5A+B} Z(\Phi) F^{tr} \right) &= 0 \\ e^{-5A(r)-B(r)} \partial_r \left(e^{3A(r)+B(r)} \partial_r\Phi \right) &= \frac{\partial V}{\partial\Phi} + 2\frac{\partial Z}{\partial\Phi} F_{tr}F^{tr}. \end{aligned} \tag{A.7}$$

We can easily solve the Gauss Law constraint for $Z(\Phi)F^{tr}$ in the third line of (A.7) to get

$$Z(\Phi)F^{tr} = Qe^{-5A(r)-B(r)} \tag{A.8}$$

where Q is the total charge of the solution. Substituting the result into the first line of (A.7) determines F_{tr} in terms of $A(r)$, $B(r)$ and their first and second derivatives. To be specific

$$F_{tr} = -\frac{e^{3A(r)+B(r)}}{2Q} (3A'(r)B'(r) + B'(r)^2 + B''(r)) + 2\lambda L^2 \frac{e^{A(r)+B(r)}}{2Q} A' [B' (A'^2 + A'B' + 2A'') + A'(r)B''(r)] \quad (\text{A.9})$$

We can then use the solution (A.9) to solve for $Z(\Phi(r))$ from (A.8),

$$Z(\Phi) = \frac{2Q^2 e^{-4A(r)}}{(3A'B' + B'^2 + B'') - 2\lambda L^2 e^{-2A(r)} A'(r) [B'(r) (A'(r)^2 + A'(r)B'(r) + 2A''(r)) + A'B'']} \quad (\text{A.10})$$

In addition, note that the second line of (A.7) gives a solution for $\partial_r \Phi$ in terms of the metric functions $A(r)$, $B(r)$, *i.e.*,

$$\Phi'(r) = \sqrt{3(1 - 2\lambda L^2 e^{-2A(r)} A'(r)^2) (A'(r)^2 + A'(r)B'(r) - A''(r))}. \quad (\text{A.11})$$

Eq. (A.11) can in principle be integrated to give an expression for $\Phi(r)$ in terms of the radial variable. Then it can be inverted to express r in terms of Φ and determine $Z(\Phi)$. Finally, substituting (A.11) together with (A.9) and (A.10) into the last line of (A.7) an expression for $\frac{\partial V}{\partial r}$ in terms of $A(r)$, $B(r)$ can be easily determined. Simply rewrite the derivatives in terms of Φ in (A.7) as $\frac{\partial}{\partial \Phi} = \frac{1}{\Phi'(r)} \frac{\partial}{\partial r}$ and solve for $\frac{\partial V}{\partial r}$ in (A.7).

It is clearly not very difficult to produce solutions of the type (A.6) from the action (A.1). Not all of these solutions however are necessarily consistent either as gravitational solutions or as dual descriptions of quantum field theories. Absence of singularities, appropriate fall-off conditions for the fields, etc. restrict the set of consistent solutions. One of the simplest consistency checks, is the null energy condition

$$T_{\mu\nu}^m u^\mu u^\nu \geq 0, \quad (\text{A.12})$$

where u^μ is an arbitrary null vector of the spacetime (A.6), *i.e.*, $g_{\mu\nu} u^\mu u^\nu = 0$. For the metric in (A.6) the null energy condition essentially amounts to requiring the first and second line of (A.7) to be non-negative

$$T_t^{t,m} - T_i^{i,m} \leq 0 \quad T_r^{r,m} - T_t^{t,m} \geq 0. \quad (\text{A.13})$$

We will now focus on a specific choice of metric which belongs to the class of metrics described by (A.6) and violates hyperscaling (for more details on these solutions and their condensed matter applications see [8-21])

$$ds^2 = r^{-2(3-\theta)/3} \left(dr^2 - r^{-2(z-1)} dt^2 + dx_i^2 \right). \quad (\text{A.14})$$

The starting point will be to analyze the null energy condition (A.13). Substituting the expressions for $A(r)$, $B(r)$ from (A.14) in (A.13) yields

$$\begin{aligned} \frac{(\theta-3)}{3} r^{\frac{-2\theta}{3}} (3+\theta-3z) \left(1 - \frac{2}{9} \lambda L^2 (\theta-3)^2 r^{\frac{-2\theta}{3}} \right) &\geq 0 \\ (z-1)(3-\theta+z) r^{\frac{-2\theta}{3}} \left(1 + \frac{2}{27} \lambda L^2 r^{\frac{-2\theta}{3}} \frac{(\theta-3)^2 (\theta-6-3z)}{3-\theta+z} \right) &\geq 0. \end{aligned} \quad (\text{A.15})$$

To determine the allowed range of values for the parameters (θ, z) from (A.15) we make the following assumptions:

- 1 that (A.14) is meaningful for all r , ranging from zero to very large values and
- 2 that the theory is also consistent at the $\lambda = 0$ point.

Eq. (A.14) then reduces to

$$\begin{aligned} (\theta-3)(3-3z+\theta) &\geq 0 & \lambda &\leq 0 \\ (z-1)(3-\theta+z) &\geq 0 & \frac{\theta-6-3z}{3-\theta+z} &\leq 0 \end{aligned} \quad (\text{A.16})$$

The left column of (A.16) provides the constraints on θ, z obtained from the null energy condition in the case of Einstein-Hilbert gravity. It is easy to see that the right column does not yield additional constraints on θ, z . It only restricts the value of the Gauss-Bonnet λ coupling to be negative.

It is clear that the geometry of (2.5) produced by taking the double-scaling limit (2.4) remains a solution of Gauss-Bonnet gravity. The null energy condition in this case yields $\lambda L^2 \leq \frac{9}{2}$.

A.2. Holographic entanglement entropy and hyperscaling violation in GB gravity

In the following we compute holographic entanglement entropy in the GB gravity. We restrict to 3+1 dimensional boundary (so that the GB term does not vanish in the bulk). We will consider the general form of the metric (A.6). The example of a metric that

violates hyper scaling is given by (A.14). The holographic entanglement entropy is equal to the extremal value of the action

$$S = \int d^3x \sqrt{\det G_\Sigma} (1 + \lambda R_\Sigma) \quad (\text{A.17})$$

where G_Σ is the induced metric.

We consider the case of a slab as defined in section 2, with induced metric

$$ds_\Sigma^2 = r^{-2(3-\theta)/3} ((1 + (x')^2) dr^2 + dx_2^2 + dx_3^2) \quad (\text{A.18})$$

where we defined $x \equiv x_1$. In this case the action (A.17) reduces to

$$S = \int dr e^{3A(r)} \sqrt{(1 + (x')^2)} \left(1 - \frac{2\lambda e^{-2A(r)} [A'(r)^2 (1 + (x')^2) + 2(1 + (x')^2) A''(r) - A'(r)(x'^2)']}{(1 + (x')^2)^2} \right) \quad (\text{A.19})$$

One can solve for x' and expand near the boundary $x = 0$

$$x'^2 = \frac{81r_0^{2\theta-6} r^{6-\frac{2\theta}{3}} \left(1 + \frac{9r^{2\theta/3}}{\lambda(\theta-3)^2} \right)}{4\lambda^2(\theta-3)^4} + \dots \quad (\text{A.20})$$

For $0 \leq \theta \leq 3$, x'^2 does not contribute to the UV (small r) divergence of (A.19).

The most interesting divergence in (A.19) comes from the $e^{3A(r)}$ term and gives rise to the $S \simeq (\epsilon/\ell)^{\theta-2}$ behavior, similarly to the Einstein-Hilbert case. The case $\theta = d - 1 = 2$ gives rise to a logarithmic term, $S \simeq \log \ell/\epsilon$, just as it did in the Einstein-Hilbert ($\lambda = 0$) case. Interestingly, in the Gauss-Bonnet case there are terms proportional to λ which exhibit stronger divergence, $S \simeq (\epsilon/\ell)^{\frac{\theta}{3}-2}$. Such terms, however, do not produce logarithmic violations of the entanglement entropy. Moreover, they are expected to vanish when the contribution from the boundary term neglected in (A.17) is included.

References

- [1] S. Sachdev, “The Quantum phases of matter,” [arXiv:1203.4565 [hep-th]].
- [2] H. Liu, J. McGreevy and D. Vegh, “Non-Fermi liquids from holography,” Phys. Rev. D **83**, 065029 (2011). [arXiv:0903.2477 [hep-th]].
- [3] M. Cubrovic, J. Zaanen and K. Schalm, “String Theory, Quantum Phase Transitions and the Emergent Fermi-Liquid,” Science **325**, 439 (2009). [arXiv:0904.1993 [hep-th]].
- [4] T. Faulkner, H. Liu, J. McGreevy and D. Vegh, “Emergent quantum criticality, Fermi surfaces, and AdS(2),” Phys. Rev. D **83**, 125002 (2011). [arXiv:0907.2694 [hep-th]].
- [5] S. S. Gubser and F. D. Rocha, “Peculiar properties of a charged dilatonic black hole in AdS_5 ,” Phys. Rev. D **81**, 046001 (2010). [arXiv:0911.2898 [hep-th]].
- [6] S. S. Gubser and J. Ren, “Analytic fermionic Green’s functions from holography,” [arXiv:1204.6315 [hep-th]].
- [7] O. DeWolfe, S. S. Gubser and C. Rosen, “Fermi surfaces in N=4 Super-Yang-Mills theory,” [arXiv:1207.3352 [hep-th]].
- [8] L. Huijse, S. Sachdev and B. Swingle, “Hidden Fermi surfaces in compressible states of gauge-gravity duality,” Phys. Rev. B **85**, 035121 (2012). [arXiv:1112.0573 [cond-mat.str-el]].
- [9] M.M. Wolf, ”Violation of the entropic area law for fermions,” Phys. Rev. Lett. **96** (2006) 010404; D. Gioev and I. Klich, ”Entanglement entropy of fermions in any dimension and the Widom conjecture,” Phys. Rev. Lett. **96** (2006) 100503.
- [10] B. Swingle, “Entanglement Entropy and the Fermi Surface,” [arXiv:0908.1724 [cond-mat.str-el]].
- [11] Y. Zhang, T. Grover and A. Vishwanath, “Topological Entanglement Entropy of Z2 Spin liquids and Lattice Laughlin states,” Phys. Rev. B **84**, 075128 (2011). [arXiv:1106.0015 [cond-mat.str-el]].
- [12] W. Ding, A. Seidel, and K. Yang, ”Entanglement Entropy of Fermi Liquids via Multi-dimensional Bosonization,” [arXiv:1110.3004 [cond-mat.stat-mech]].
- [13] S. Ryu and T. Takayanagi, “Holographic derivation of entanglement entropy from AdS/CFT,” Phys. Rev. Lett. **96**, 181602 (2006). [hep-th/0603001].
- [14] S. Ryu and T. Takayanagi, “Aspects of Holographic Entanglement Entropy,” JHEP **0608**, 045 (2006). [hep-th/0605073].
- [15] N. Ogawa, T. Takayanagi and T. Ugajin, “Holographic Fermi Surfaces and Entanglement Entropy,” JHEP **1201**, 125 (2012). [arXiv:1111.1023 [hep-th]].
- [16] E. Shaghoulian, “Holographic Entanglement Entropy and Fermi Surfaces,” JHEP **1205**, 065 (2012). [arXiv:1112.2702 [hep-th]].
- [17] X. Dong, S. Harrison, S. Kachru, G. Torroba and H. Wang, “Aspects of holography for theories with hyperscaling violation,” JHEP **1206**, 041 (2012). [arXiv:1201.1905 [hep-th]].

- [18] K. Narayan, “On Lifshitz scaling and hyperscaling violation in string theory,” *Phys. Rev. D* **85**, 106006 (2012). [arXiv:1202.5935 [hep-th]].
- [19] B. S. Kim, “Schrödinger Holography with and without Hyperscaling Violation,” *JHEP* **1206**, 116 (2012). [arXiv:1202.6062 [hep-th]].
- [20] K. Hashimoto and N. Iizuka, “A Comment on Holographic Luttinger Theorem,” [arXiv:1203.5388 [hep-th]].
- [21] E. Perlmutter, “Hyperscaling violation from supergravity,” *JHEP* **1206**, 165 (2012). [arXiv:1205.0242 [hep-th]].
- [22] M. Cadoni and S. Mignemi, “Phase transition and hyperscaling violation for scalar Black Branes,” *JHEP* **1206**, 056 (2012). [arXiv:1205.0412 [hep-th]].
- [23] M. Ammon, M. Kaminski and A. Karch, “Hyperscaling-Violation on Probe D-Branes,” [arXiv:1207.1726 [hep-th]].
- [24] J. Bhattacharya, S. Cremonini and A. Sinkovics, “On the IR completion of geometries with hyperscaling violation,” [arXiv:1208.1752 [hep-th]].
- [25] N. Kundu, P. Narayan, N. Sircar and S. P. Trivedi, “Entangled Dilaton Dyons,” [arXiv:1208.2008 [hep-th]].
- [26] S. A. Hartnoll and E. Shaghoulian, “Spectral weight in holographic scaling geometries,” [arXiv:1203.4236 [hep-th]].
- [27] D. J. Gross and H. Ooguri, “Aspects of large N gauge theory dynamics as seen by string theory,” *Phys. Rev. D* **58**, 106002 (1998). [hep-th/9805129].
- [28] K. Zarembo, “Wilson loop correlator in the AdS / CFT correspondence,” *Phys. Lett. B* **459**, 527 (1999). [hep-th/9904149].
- [29] P. Olesen and K. Zarembo, “Phase transition in Wilson loop correlator from AdS / CFT correspondence,” [hep-th/0009210].
- [30] H. Kim, D. K. Park, S. Tamarian and H. J. W. Muller-Kirsten, “Gross-Ooguri phase transition at zero and finite temperature: Two circular Wilson loop case,” *JHEP* **0103**, 003 (2001). [hep-th/0101235].
- [31] T. Hirata and T. Takayanagi, “AdS/CFT and strong subadditivity of entanglement entropy,” *JHEP* **0702**, 042 (2007). [hep-th/0608213].
- [32] A. Pakman and A. Parnachev, “Topological Entanglement Entropy and Holography,” *JHEP* **0807**, 097 (2008). [arXiv:0805.1891 [hep-th]].
- [33] D. V. Fursaev, “Proof of the holographic formula for entanglement entropy,” *JHEP* **0609**, 018 (2006). [hep-th/0606184].
- [34] J. de Boer, M. Kulaxizi and A. Parnachev, “Holographic Entanglement Entropy in Lovelock Gravities,” *JHEP* **1107**, 109 (2011). [arXiv:1101.5781 [hep-th]].
- [35] L. -Y. Hung, R. C. Myers and M. Smolkin, “On Holographic Entanglement Entropy and Higher Curvature Gravity,” *JHEP* **1104**, 025 (2011). [arXiv:1101.5813 [hep-th]].

- [36] M. Alishahiha, M. R. M. Mozaffar and A. Mollabashi, “Holographic Aspects of Two-charged Dilatonic Black Hole in AdS5,” [arXiv:1208.2535 [hep-th]].
- [37] M. Taylor, “Non-relativistic holography,” [arXiv:0812.0530 [hep-th]].
- [38] K. Goldstein, N. Iizuka, S. Kachru, S. Prakash, S. P. Trivedi and A. Westphal, “Holography of Dyonically Dilaton Black Branes,” JHEP **1010**, 027 (2010). [arXiv:1007.2490 [hep-th]].
- [39] C. Charmousis, B. Gouteraux, B. S. Kim, E. Kiritsis and R. Meyer, “Effective Holographic Theories for low-temperature condensed matter systems,” JHEP **1011**, 151 (2010). [arXiv:1005.4690 [hep-th]].
- [40] M. Cadoni and P. Pani, “Holography of charged dilatonic black branes at finite temperature,” JHEP **1104**, 049 (2011). [arXiv:1102.3820 [hep-th]].
- [41] B. Gouteraux and E. Kiritsis, “Generalized Holographic Quantum Criticality at Finite Density,” JHEP **1112**, 036 (2011). [arXiv:1107.2116 [hep-th]].
- [42] M. Cvetič, M. J. Duff, P. Hoxha, J. T. Liu, H. Lu, J. X. Lu, R. Martinez-Acosta and C. N. Pope *et al.*, “Embedding AdS black holes in ten-dimensions and eleven-dimensions,” Nucl. Phys. B **558**, 96 (1999). [hep-th/9903214].
- [43] I. R. Klebanov, D. Kutasov and A. Murugan, “Entanglement as a probe of confinement,” Nucl. Phys. B **796**, 274 (2008). [arXiv:0709.2140 [hep-th]].
- [44] H. Liu and M. Mezei, “A Refinement of entanglement entropy and the number of degrees of freedom,” [arXiv:1202.2070 [hep-th]].
- [45] R. C. Myers and A. Singh, “Comments on Holographic Entanglement Entropy and RG Flows,” JHEP **1204**, 122 (2012). [arXiv:1202.2068 [hep-th]].
- [46] N. Ogawa and T. Takayanagi, “Higher Derivative Corrections to Holographic Entanglement Entropy for AdS Solitons,” JHEP **1110**, 147 (2011). [arXiv:1107.4363 [hep-th]].
- [47] M. Brigante, H. Liu, R. C. Myers, S. Shenker and S. Yaida, “Viscosity Bound Violation in Higher Derivative Gravity,” Phys. Rev. D **77**, 126006 (2008). [arXiv:0712.0805 [hep-th]].
- [48] M. Brigante, H. Liu, R. C. Myers, S. Shenker and S. Yaida, Phys. Rev. Lett. **100**, 191601 (2008). [arXiv:0802.3318 [hep-th]].
- [49] A. Buchel and R. C. Myers, “Causality of Holographic Hydrodynamics,” JHEP **0908**, 016 (2009). [arXiv:0906.2922 [hep-th]].
- [50] D. M. Hofman, “Higher Derivative Gravity, Causality and Positivity of Energy in a UV complete QFT,” Nucl. Phys. B **823**, 174 (2009). [arXiv:0907.1625 [hep-th]].
- [51] T. Nishioka and T. Takayanagi, “AdS Bubbles, Entropy and Closed String Tachyons,” JHEP **0701**, 090 (2007). [hep-th/0611035].
- [52] H. Casini and M. Huerta, “Entanglement entropy in free quantum field theory,” J. Phys. A **42**, 504007 (2009). [arXiv:0905.2562 [hep-th]].

- [53] I. R. Klebanov, T. Nishioka, S. S. Pufu and B. R. Safdi, “On Shape Dependence and RG Flow of Entanglement Entropy,” JHEP **1207**, 001 (2012). [arXiv:1204.4160 [hep-th]].